Mechanical measurement of the residual stress in thin PVD films

ELSEVIER

Thin Solid Films 270 (1995) 264–269

thin solid films

Mechanical measurement of the residual stress in thin PVD films

R.O.E. Vijgen, J.H. Dautzenberg

Eindhoven, University of Technology, Department of Mechanical Engineering, P.O. Box 513 5600 MB Eindhoven, The Netherlands

Abstract

A practical mechanical bending plate method is proposed to calculate the residual stress present in thin physical vapour deposition films. A thin circular foil of stainless steel is coated with TiN, using an unbalanced magnetron sputtering technique. Sectioning of this foil into narrow strips leads to an easily measurable radius of curvature. With the help of calculations based on the finite element method it is shown that, if the width-to-length ratio is small, the analytical formula of Senderoff is valid. Above a certain width-to-length ratio, serious errors in calculated stress values are introduced using Senderoff. The second part of this paper describes the influences of the deposition parameters of TiN on the residual stress in the coating. An increase of the bias voltage results in a higher compressive stress, varying from −4.2 to −7.2 GPa. Experiments with different substrate materials show that the growth stress is independent of the substrate material. The total residual stress present in the coating increases with a higher magnetron current and a lower working gas pressure.

There was excellent agreement between the results of the proposed method and X-ray diffraction (Seemann–Bohlin).

Keywords: Stress; Physical vapour deposition; Steel; Titanium nitride

1. Introduction

Residual stresses in coatings influence the mechanical properties such as hardness, fracture strain and adherence [1,2]. These stresses arise because of the expansion mismatch between the coating and the substrate exposed to a temperature gradient (thermomechanical stresses) and growth stresses. The growth stress originates from rapid solidification and intense ion bombardment. Both phenomena result in all kinds of lattice imperfections [3]. Residual stresses can be measured with a X-ray diffraction (XRD) [4,5] or a mechanical "bending plate method" [6,7]. The XRD method is based on measurement of the change in the lattice plane distance of a certain *hkl* plane set for different orientations of the specimen [8]. With the bending plate method the change in curvature of a substrate is measured which is a result of the present residual stress in the deposited coating. This method is preferred to XRD because of the practical use in the job-coat industry. The choice of the relation between substrate deformation and coating stress depends on the maximum substrate deflection. If the maximum mid-plain deflection is in the order of the plate thickness, the relations based on the plate theory of Kirchhoff are used. Such small deflections, however, require an accurate measuring system leading to time consumable displacement analyses. In the case of large deflections, Senderoff's stress formulas are used (Appendix A), which are based on the elastic beam theory [9].

This theory is only applicable if the width-to-length ratio of the substrate is small. The validity of Senderoff's formula, regarding the substrate geometry used, is checked by means of the finite element method (FEM).

This paper describes a method that can easily be used in the job-coat industry. Results are presented of the calculated residual stress of TiN as a function of the substrate material, the bias voltage, the magnetron current and the argon pressure. The calculated residual stresses obtained from the bending foil method are compared with the XRD stress analysis.

2. Experimental set-up

All coatings are produced with a Teer UDP 350 4-RF system [10] using 4 unbalanced magnetrons (Type II), a closed magnetic field configuration, an optical gas control and a radio frequency (r.f.) bias supply. The TiN coatings are deposited on a stationary substrate, using only 1 magnetron. In all experiments the distance substrate–target (D_{st}) was 130 mm.

The standard coating cycle (Table 1) consists of a cleaning procedure, a deposition stage and a cooling down period. During sputter cleaning the bias voltage was −1000 V and the magnetron was set to a constant current of 0.2 A. This

SSDI 0040-6090(95)06984-4

Table 1
The standard coating cycle of a TiN coating. The run consists of a cleaning procedure, a deposition stage and a cooling down period

Cleaning procedure
15 min ultrasonic cleaning in alcohol
Pumping down vacuum chamber until $p < 10^{-2}$ Pa
Inlet of argon until $P = 0.3$ Pa
30 min sputter cleaning
bias voltage, $V_b = -1000$ V; magnetron current, $I_{mag} = 0.2$ A
Deposition stage
Bias voltage, $V_b = -150$ V; magnetron current, $I_{mag} = 7.5$ A
Inlet of nitrogen
Decrease of V_b to the desired value
Cooling down

way more ions were ejected into the plasma leading to a higher cleaning efficiency. Furthermore, the target was cleaned and residual oxygen is gettered by the metal. In the deposition stage the bias voltage was decreased down to -150 V and a metallic titanium coating of approximately 50 nm deposited by increasing the current of the magnetron to the desired value (normally 7.5 A). The titanium intensity (I_0) was measured with an optical emission monitor and set to I (55% of the initial value of I_0). Inlet of nitrogen decreases the intensity from I_0 to I. After the intensity of titanium was set, the bias voltage decreased to the desired value and held constant during the deposition of TiN. For all reported experiments it has to be mentioned that no parameter was changed during the deposition of TiN. The chemical composition of the produced coatings ranges from $Ti_{0.52}N_{0.48}$ up to $Ti_{0.53}N_{0.47}$ (Rutherford backscattering spectroscopy (RBS) measurements).

A circular thin foil (substrate, thickness 70 μm) was mounted in a substrate holder. A chamber was machined into the holder that allowed the substrate to move in a radial direction (Fig. 1). Shortly after TiN deposition, the temperature was measured with a calibrated infrared temperature monitor.

Due to concentricity of the substrate and coating no remarkable bending occurred. The circular substrate was sectioned into small rectangular strips (beams) with a width of 0.2 mm and a length of 30 mm, using a shearing machine. The radius of curvature was measured with a calibrated overhead projector (Appendix B). The coating thickness was measured with a modified ball crater method (Appendix B) using an electro-sparking machine. The depth of the eroded hole greatly influences the accuracy of the measured coating thickness. Using this equipment results in the accurate obtainment of the prescribed erosion depth. An error analysis of the used method was performed (Appendix B) and applied to all the measurements. The estimated error ($\pm S_\sigma$) is presented in the figures as an error bar.

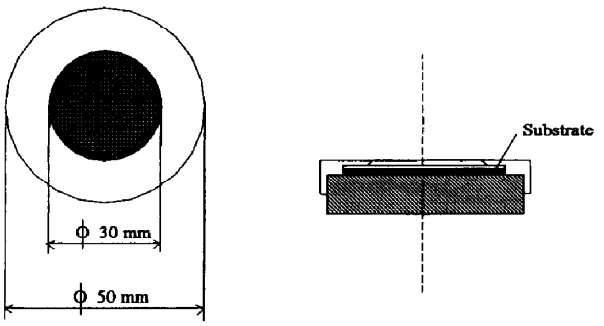

Fig. 1. Schematic drawing of the substrate holder used.

3. Results

The validity of Senderoff's theory, with respect to the width-to-length ratio (w/l), is checked with the help of finite element calculations. In Fig. 2, the radius of curvature is shown as a function of the width-to-length ratio of a 75 μm thick substrate made of stainless steel. The initial stress in a 1.65 μm thick TiN coating is -5.3 GPa applied in two-dimensions parallel to the surface. The physical constants used are summarised in Table 2 [11–13]. It is evident from this figure that the radius of curvature remains constant below a width-to-length ratio (w/l) of 0.07. Comparison of the results of Senderoff's model and the finite element calculations gives excellent agreement for a width-to-length ratio below 0.07. Above this value, serious errors are introduced with regard to the calculated stress using this analytical formula.

The total residual stress is the sum of the growth stresses and the thermomechanical stress. To investigate the influence of the substrate material on the stresses three different materials are coated with a 1.25 μm thick TiN coating (bias voltage, $V_b = -65$ V; magnetron current, $I_{mag} = 7.5$ A; working gas pressure ,$P_{Ar} = 0.3$ Pa).

The temperature during the deposition process ranged from 250 °C (end of the cleaning stage) to 300 °C (end of the deposition stage). The thermomechanical stress was calculated with the formulas of Hsueh and Evans [14]. The results are represented in Fig. 3. From this figure it can be concluded that the growth stress is independent of the substrate material.

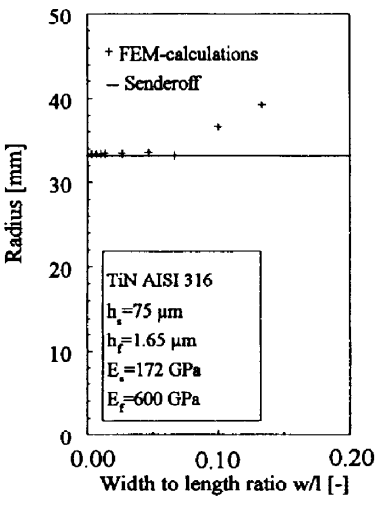

Fig. 2. Comparison of the calculated radius of curvature obtained by finite element calculations and Senderoff's formula.

Furthermore thermomechanical stresses (in the order of 1 GPa) have a minor contribution to the total residual stress (in the order of 6 GPa).

Increase of the bias voltage from 20 V to 150 V ($I_{mag}=7.5$ A, $P_{Ar}=0.3$ Pa) results in a larger compressive stress (Fig. 4). This behaviour is explained by the higher kinetic energy of the bombarding Ar^+ ions on the substrate with increasing bias voltage. Changing the magnetron current from 4 to 6 A ($V_b=-65$ V, $P_{Ar}=0.3$ Pa) results in a constant

Table 2
The Young's modulus E, the Poisson's ratio ν and the linear expansion coefficient α of the used substrate materials and the TiN coating [11–13]

	E (GPa)]	$\alpha x10^{-6}$ ($°C^{-1}$)	ν
AISI 316	177	16.2	0.3
Molybdenum	325	5.5	0.28
Tungsten	405	4.4	0.28
TiN	600	9.4	0.25

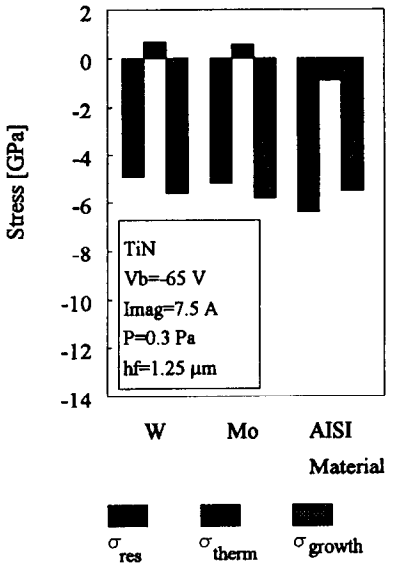

Fig. 3. Total residual stress σ_{res}, thermomechanical stress σ_{therm} and growth stress σ_{growth} of TiN as a function of the substrate material.

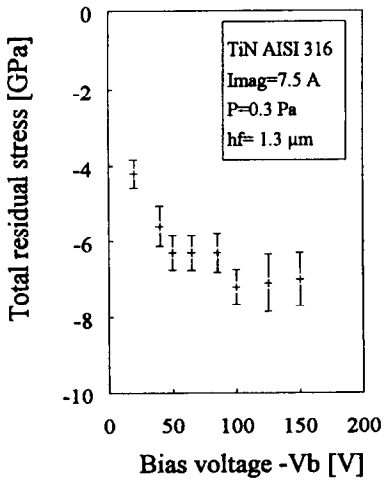

Fig. 4. Total residual stress of TiN vs. the bias voltage V_b.

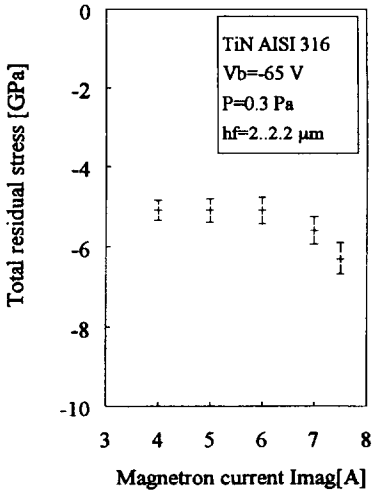

Fig. 5. Total residual stress of TiN vs. the magnetron current (I_{mag}).

Table 3
The growth stress σ_{growth} of TiN as a function of the magnetron current I_{mag}

I_{mag} (A)	σ_{res} (GPa)	σ_{growth} (GPa)	N_i/N_m	$\sigma_{growth}/(N_i/N_m)$
4	−5.1	−4.5	2.6	−1.7
5	−5.1	−4.5	2.6	−1.7
6	−5.2	−4.6	2.6	−1.8
7	−5.6	−5.0	2.8	−1.8
7.5	−6.4	−5.5	2.9	−1.9

σ_{res}, total residual stress; σ_{growth}, growth stress; N_i/N_m, substrate ion-to-metal arrival rate.

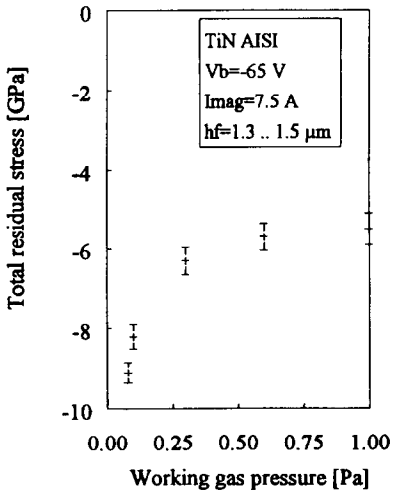

Fig. 6. Total residual stress of TiN vs. the working gas pressure.

total residual stress (Fig. 5). Above a magnetron current of 6 A, the compressive stress in the coating increases with higher magnetron current. The growth stress as a function of the magnetron current also increases above $I_{mag}=6$ A (Table 3). This increase is a result of the higher ion-to-metal arrival rate N_i/N_m.

Decrease of the working gas pressure below a value of 0.3 Pa (Fig. 6) results in a large increase in the total residual stress ($V_b=-65$ V, $I_{mag}=7.5$ A). This behaviour might be explained by a decrease of gas scattering with lower gas

pressure, leading to more energetic ions with a higher kinetic energy.

4. Discussion

First of all, it should be stated that the calculated residual stress is an average value, assuming that no stress gradient perpendicular to the interface is present.

The error propagation of this test method is illustrated by the following example. An approximately 1 μm thick TiN coating was deposited on a 70 μm thick stainless steel foil.

The radius of curvature measured with the overhead projector was 26.1 ± 1.3 mm ($R \pm S_R$). Using the ball crater method a layer thickness of 1.45 ± 0.08 was measured. Substitution of these values in Eq. (A1) (Appendix A) and, respectively, Eq. (A6) (Appendix B), result in a total residual stress value of 6.6 ± 0.4 GPa (for details see Appendix B). Fig. 7 shows the total residual stress measured for eight different test pieces produced at the same deposition parameters.

XRD stress analyses are carried out to check the bending foil method. The Seemann Bohlin geometry was used because of the low penetration depth of the X-rays [5]. The residual stress was measured from three different TiN coatings with this method at the Bergakademie Freiberg, Germany. A comparison of the results of both methods showed good agreement (Table 4).

FEM calculations were carried out to investigate the influence of plastic deformation of the substrate on the curvature of the beam. In Fig. 8 the curvature is plotted vs. the total residual stress. Above approximately 3 GPa, plastic deformation occurs leading to an increase in curvature. However, stripping off the coating leads to a flat substrate indicating that no plastic deformation has taken place. The difference between the calculations and experiments might be explained by the high flow stress of the substrate material caused by cold rolling.

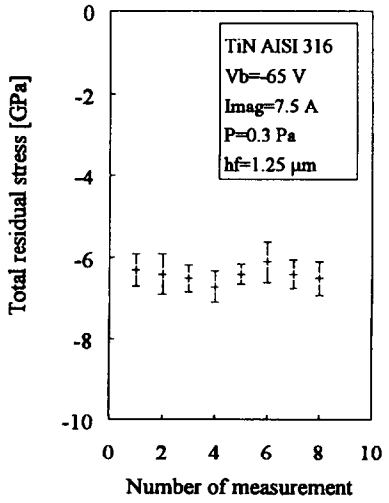

Fig. 7. Variation of the total residual stress.

Table 4
Comparison of the total residual stress of TiN obtained with the bending foil and the XRD method for three different bias voltages

Bias voltage (V)	Bending foil method (GPa)	XRD method (GPa)
−20	−4.2	−3.9
−65	−6.4	−5.8
−150	−7.0	−6.8

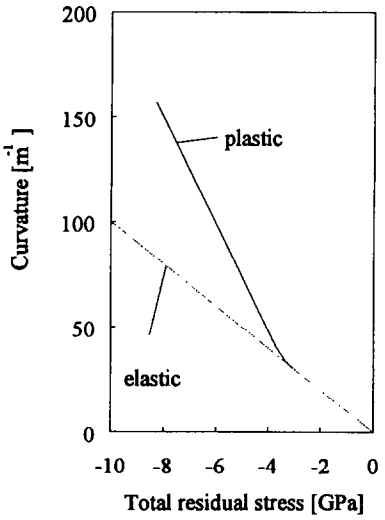

Fig. 8. Influence of plastic deformation of the substrate on the curvature of the beam. (material AISI 316 characteristic stress $C = 1400$, the strain-hardening exponent $n = 0.5$ and the pre-strain $\epsilon_0 = 0.037$).

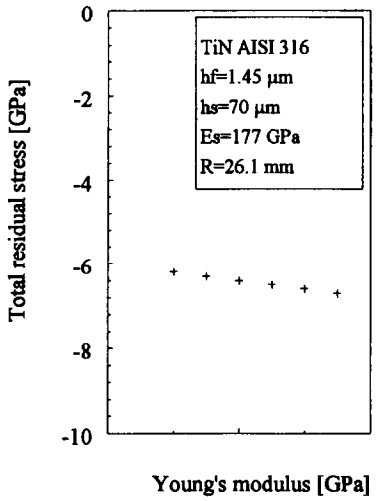

Fig. 9. The total residual stress as a function of Young's modulus of the coating.

The Young's modulus of the coating is taken from the literature ($E_{TiN} = 600$ GPa). This value might be too high or may vary with the deposition parameters. Initial calculations of the Young's modulus of TiN, using the nano-indentation technique [15], resulted in a value of 577 GPa. This result agrees well with work carried out by Wang [16]. However, more research has to be done on this subject. In order to give an indication for the introduced error in the total residual stress, calculations were performed with different values of the Young's modulus of coating. In Fig. 9, the results are

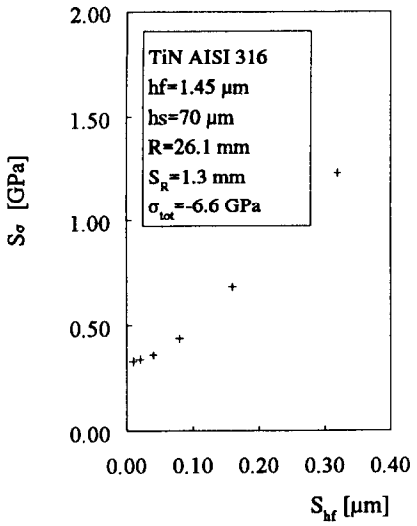

Fig. 10. The experimental error of the total residual stress (S_σ) as a function of the experimental error of the measured coating thickness (S_{hf}).

presented for a 1.65 μm thick coating deposited on a 75 μm stainless steel substrate with a radius of curvature of 34 mm. Varying the Young's modulus of TiN from 400 to 650 GPa results in a stress value of −6.2 GPa to −6.7 GPa. This result indicates that the variation of the TiN Young's modulus is of minor interest. Errors introduced by coating thickness measurements result in large errors in the calculated stress (Fig. 10). This error diminishes as the coating thickness becomes larger.

The trend in the total residual stress as a function of the bias voltage and the substrate ion-to-neutral ratio (magnetron current) is also observed by Musil et al. [17]. They related the residual stress to the deposition parameter E_p, which is proportional to the product of the bias voltage and the substrate ion-to-metal arrival rate. The increase in total residual stress of our experiments takes place at an E_p of 150 eV atom^{-1}. This increase corroborates the work proposed by Musil et al. However, below an E_p of 150 eV atom^{-1} they found a tensile stress present in the coating and related this to the porous coating structure. Similar behaviour regarding the transition from porous to dense ($E_p > 150$ eV atom^{-1}) was found in our experiments. The value of the calculated stresses, however, differs and might be a result of the compressive stress present in the columns of the TiN coating.

The trend of the total residual stress as a function of the working gas pressure is similar to the work presented by Cerny et al. [18].

5. Conclusions

An accurate and practical method is presented to measure the residual stresses of thin films. A comparison between the finite element analysis and Senderoff's model shows an excellent agreement if the width-to-length ratio is small ($w/l < 0.07$). Above this value, serious errors are introduced.

There was excellent agreement between the results obtained with the bending foil method and the XRD method. The total error of the proposed method is mainly determined by the error introduced by the film thickness measurement (S_{hf}).Experiments with different substrate materials show a constant growth stress.

Increase of the bias voltage results in a higher residual stress. An abrupt increase in growth stress is found if the magnetron current is increased from 6 to 7.5 A. The growth stress is proportional to the ratio of the ion current density and the deposition rate. Both trends can be explained by the deposition parameter E_p proposed by Musil et al. [17]. The total residual stress decreases with higher discharge pressure.

Appendix A. Senderoff's formula

The total residual stress was calculated using Senderoff's formula:

$$\sigma_{res} = \frac{\dfrac{E_s}{(1-\nu_s)}\left(h_s + \dfrac{E_c(1-\nu_s)}{E_s(1-\nu_c)}h_f\right)^3}{6Rh_sh_f} \quad \text{(A1)}$$

where σ_{res} is the total residual stress (GPa), E_c the Young's modulus of the coating (GPa), E_s the Young's modulus of the substrate (GPa), ν_c the Poisson's ratio of the coating, ν_s the Poisson's ratio of the substrate, h_s the thickness of the substrate (m), h_f the thickness of the coating (m), and R the radius of curvature (m).

Appendix B. Error analysis of the used bending foil method

The radius of curvature was measured with an overhead projector (magnification 20). By measuring a and d_f (Fig. 11) the radius of curvature R was calculated using:

$$R = \frac{d_f^2 + a^2}{2d_f} \quad \text{(B1)}$$

where R is the radius of curvature (mm), d_f the deflection (mm) (see Fig. 11), and a the distance (mm) (see Fig. 11).

The experimental error of the radius measurement is:

$$S_R = \sqrt{\left(\frac{a^2}{d_f^2}S_{d_f}^2 + \left(1 - \frac{d_f^2 + a^2}{2d_f^2}\right)S_a^2\right)} \quad \text{(B2)}$$

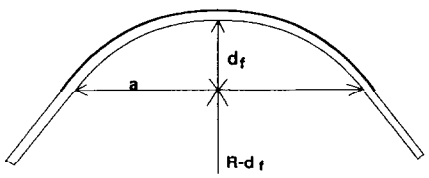

Fig. 11. Schematic drawing of the bent beam, showing the parameter d_f, a and the radius of curvature R.

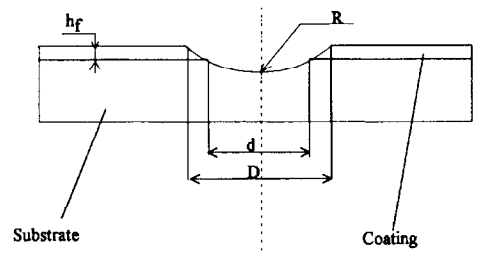

Fig. 12. Schematic drawing of an eroded hole, showing the ball radius r, the inner diameter d, the outer diameter D and the coating thickness h_f.

where S_R is the experimental error of the radius measurement (mm), S_{d_f} the experimental error in measuring d_f (mm), and S_a the experimental error in measuring a (mm).

The coating thickness h_f was measured with a modified ball crater technique. A ball is electro-machined into the coating/substrate (Fig. 12).

$$h_f = \sqrt{(r^2 - 1/4d^2)} - \sqrt{(r^2 - 1/4D^2)} \quad \text{(B3)}$$

where h_f is the coating thickness (μm), r the radius of the sparking ball (μm), d the inner diameter of the sparked hole (μm), and D the outer diameter of the sparked hole (μm).

The experimental error of this technique was calculated using the following formula:

$$S_{h_f} = \sqrt{\left(\left(\frac{1}{4}\frac{S_d^2 d^2}{4R^2 - d^2}\right) + \left(\frac{1}{4}\frac{S_D^2 D^2}{2R^2 - D^2}\right)\right)} \quad \text{(B4)}$$

where S_{h_f} is the experimental error in the determination of the coating thickness (μm), S_d the experimental error in the determination of the inner diameter d (μm), and S_D the experimental error in the determination of the outer diameter D (μm).

Both mentioned errors result in the total experimental error of the bending foil method:

$$S_\sigma = \sqrt{\left(\left(\frac{E'_s\left(h_s + \frac{E'_c h_f}{E'_s}\right)^3}{6R^2 h_s h_f}\right)^2 S_R^2 + \left(\frac{E'_s\left(h_s + \frac{E'_c h_f}{E'_s}\right)^2}{2Rh_s h_f} - \frac{E_s\left(h_s + \frac{E'_c h_f}{E'_s}\right)^3}{6Rh_s h_f^2}\right)^2 S_{h_f}^2\right)} \quad \text{(B5)}$$

where S_σ is the experimental systematic error of the total residual stress (GPa), E'_c the effective Young's modulus of the coating ($E_c/(1-\nu_c)$) (GPa), E'_s the effective Young's modulus of the substrate ($E_s/(1-\nu_s)$) (GPa), h_s the thickness of the substrate (m), h_f the thickness of the coating (m), and R the radius of curvature (m).

The following example gives an indication of the error propagation.

- An approximately 1.5 μm thick TiN coating is deposited on stainless steel (70 μm).
- The radius of curvature of a sectioned beam R, and the related systematic error S_R, are calculated using Eqs. (B1) or (B2), respectively, using the following parameters: $2a^* = 401$ mm (magnification 20); $d_f^* = 40$ mm (magnification 20); $S_a = 2$ mm (magnification 20); $S_{d_f} = 2$ mm (magnification 20). Resulting in $R = 26.1$ mm and $S_R = 1.3$ mm.
- Substitution of: $D = 86 \times 2.3$ μm; $d = 29 \times 2.3$ μm; $r = 3000$ μm; $S_d = 4.6$ μm; $S_D = 4.6$ μm into Eqs. (B3) or (B4), respectively, results in a layer thickness $h_f = 1.45$ μm and an error $S_{h_f} = 0.08$ μm.

The total residual stress (Eq. (A1)) of this example is -6.6 GPa with an experimental error (Eq. (B5)) $S_\sigma = 0.4$ GPa. This error $\pm S_\sigma$ is presented in the figures as an error bar.

References

[1] R.O.E. Vijgen, M.A. Raijmakers and J.H. Dautzenberg, in B. Vorsatz and E. Szoke (eds.), *Proc. Conf. EUROMAT '94, Balatonszeplak, Hungary, 1994*, Euromat 94 Topical, Volume II, p. 488.
[2] S.J. Bull, D.S. Rickerby, A. Matthews, A. Leyland, A.R. Pace and J. Valli, *Surf. Coat. Technol., 36* (1988) 503.
[3] G. Håkansson, *Ph.D. Thesis*, Linköping University, 1991.
[4] R. Kuzel, R. Černy, V. Valvoda, M. Blomberg and M. Merisalo, *Thin Solid Films, 247* (1994) 64.
[5] A.J. Perry, V. Valvoda and D. Rafaja, *Thin Solid Films, 214* (1992) 169.
[6] D.E. Fahnline, C.B. Masters and N.J. Salamon, *J. Vac. Sci. Technol. A, 9* (1991) 2483.
[7] B.D. Harper and C.-P. Wu, *Int. J. Solid Struct., 26* (1990) 511.
[8] B.A. van Brussel, *Ph.D. Thesis*, University of Groningen, 1993.
[9] S. Senderoff and A. Brenner, *Nat. Bur. Stand., 42* (1949) 105.
[10] D.G. Teer, *Surf. Coat. Technol., 39/40* (1989) 565.
[11] E. Török, A.J. Perry, L. Chollet and W.D. Sproul, *Thin Solid Films, 153* (1987) 37.
[12] D. Peckner and I.M. Bernstein, *Handbook of Stainless Steels*, Mc Graw–Hill, New York, 1977.
[13] H.E. Howard and T.L. Gall, *Metals Handbook*, American Society for Metals, Metals Park, OH, 1985.
[14] C.H. Hsueh and A.G. Evans, *J. Am. Ceram. Soc., 68* (1985) 241.
[15] W.C. Oliver, G.M. Pharr, *J. Mater. Res., 7(6)* (1992) 1564.
[16] M. Wang, *Ph.D. Thesis*, RWTH Aachen, 1992.
[17] J. Musil, S. Kadlec, V. Valvoda, R. Kuzel and R. Cerny, *Surf. Coat. Technol., 43/44* (1990) 259.
[18] R. Cerny, R. Kuzel, V. Valvoda, S. Kadlec and J. Musil, *Surf. Coat. Technol., 64* (1994) 111.